The finite element method for the space fractional magnetohydrodynamic flow and heat transfer on an irregular domain

Yi Liu[1] Xiaoyun Jiang[2] Fawang Liu[3]

(Received 8 January 2023; revised 23 October 2023)

Abstract

We consider the magnetohydrodynamic flow and heat transfer of a classical Newtonian fluid in a straight channel with fixed irregular cross section. A spatial fractional operator is introduced to modify the classical Fourier's law of thermal conduction, and we obtain the space fractional coupled model. With the help of the finite element method, the coupled model is solved numerically. Finally, a special numerical example is proposed to verify the stability and efficiency of the presented method.

DOI:10.21914/anziamj.v64.17912, Published 2023-11-01, as part of the Proceedings of the 20th Biennial Computational Techniques and Applications Conference. ISSN 1445-8810. (Print two pages per sheet of paper.)

Contents

1 Introduction

In recent years, the magnetohydrodynamic (MHD) flow and heat transfer problem has attracted great attention due to its extensive applications in actual production and life. Because fractional operators have the characteristics of heredity and memory, they are widely used in the modelling and application of MHD flow and heat transfer. Zheng et al. [14] presented an analysis method for MHD flow of an incompressible generalized Oldroyd-B fluid. The effect of second order slip on MHD flow of a fractional Maxwell fluid was explored by Aman [1].

Due to their complexity, many numerical methods have been developed to solve fractional equations [7, 8]. Li and Zeng [9] employed finite difference methods to solve fractional differential equations. In recent years, Zhang et al. [12] developed a time-stepping numerical method for time-fractional nonlinear equations.

In this article we provide a numerical method to solve the space fractional MHD flow and heat transfer coupled model, which occurs in an irregular domain. Irregular domains are considered because flow problems in such domains have

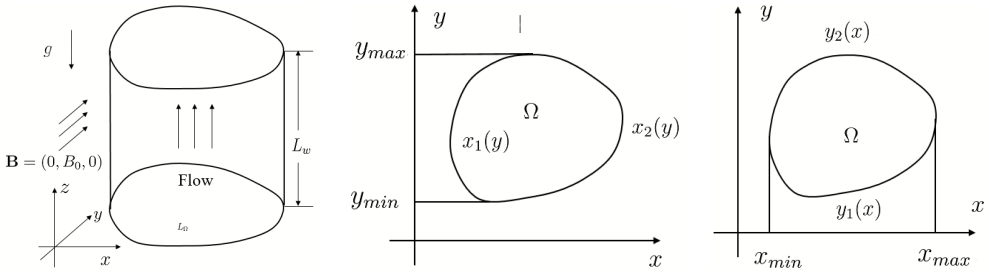

(a) Physical model (b) Convex domain (c) Convex domain

Figure 1: Physical model and convex domain Ω with boundaries $x_1(y)$, $x_2(y)$, $y_1(x)$ and $y_2(x)$.

more extensive application value. This numerical method can be used to calculate other space fractional coupled models, providing a framework for studying the MHD flow and heat transfer problems of space fractional fluid. This article is organized as follows: the space fractional coupled model is given in Section 2. Based on the unstructured finite method, Section 3 proposes the numerical method. In Section 4, we present the matrix form of the method and a numerical example is considered to verify the stability and efficiency of the numerical scheme. Section 5 presents some conclusions.

2 Mathematical model

The physical model and the convex cross sectional domain Ω are shown in Figure 1. We assume that the length of the channel L_w is in the z-direction and is much longer than the diameter of the cross sectional domain Ω which lies in the xy-plane. The channel is filled with classical Newtonian fluid. The channel wall has non-slip boundary conditions, and has constant temperature T_w. The channel and fluid are exposed to a constant magnetic field $\mathbf{B}$ in the y-direction. The flow is independent of z, that is to say, the velocity distribution of the model is $\mathbf{u} = (0, 0, w(x, y, t))$.

The momentum equations are [10]

$$\nabla \cdot \mathbf{u} = 0\,,$$
$$\rho\left[\frac{\partial \mathbf{u}}{\partial t} + (\mathbf{u}\cdot\nabla)\mathbf{u}\right] = \nabla\cdot\mathbf{S} + \mathbf{J}\times\mathbf{B} + \rho g\eta(T - T_w)\,, \tag{1}$$

where $\mathbf{u} = (0, 0, w)$ is the velocity vector, ∇ is the gradient operator, ρ is the density of the fluid, $\mathbf{S}$ is the Cauchy stress tensor, $\mathbf{g}$ is the gravitational acceleration vector, η is the coefficient of thermal expansion, and T and T_w are the temperatures of the fluid and the wall, respectively. Since the flow is subjected to an external magnetic field, we include $\mathbf{J}\times\mathbf{B}$, in which $\mathbf{J}$ is the current density vector and $\mathbf{B}$ is the total magnetic field vector. According to the characteristics of a classical Newtonian fluid, the viscous stress constitutive equations are $S_{xz} = \mu\partial w/\partial x$ and $S_{yz} = \mu\partial w/\partial y$, in which μ is the dynamic viscosity, and $S_{xx} = S_{xy} = S_{yy} = S_{zz} = 0$. The generalized Ohm's law is $\mathbf{J} + \xi(\mathbf{J}\times\mathbf{B}) = \sigma(\mathbf{E} + \mathbf{u}\times\mathbf{B})$ [4], where ξ is the Hall coefficient, $\mathbf{E}$ is the electric field, and σ is the electric conductivity. The distribution of magnetic field is $\mathbf{B} = (0, B_0, 0)$. Neglecting the effect of the electric field in the Hall effect, the governing equation (1) is transformed into

$$\frac{\partial w}{\partial t} = \frac{\mu}{\rho}\left(\frac{\partial^2 w}{\partial x^2} + \frac{\partial^2 w}{\partial y^2}\right) - \frac{\sigma B_0^2}{\rho(1+\xi^2 B_0^2)}w - g\eta(T - T_w)\,. \tag{2}$$

Due to the influence of external magnetic field, the flow is affected by the Joule heating effect. The temperature equation with the Joule heating effect is

$$\rho C_p\left[\frac{\partial T}{\partial t} + (\mathbf{u}\cdot\nabla)T\right] = -\nabla\cdot\mathbf{q} + R_J\,, \tag{3}$$

where C_p is the heat capacity, $\mathbf{q}$ is the heat flux, and the Joule heating effect is $R_J = \frac{1}{\sigma}|\mathbf{J}|^2$ [3]. We apply a new spatial fractional heat conduction model to describe the heat flux $\mathbf{q} = -k\lambda^{\alpha-1}\nabla^\alpha T$ [13]. Here k is the thermal conductivity, α is the spatial fractional derivative parameter satisfying $0 <$

$\alpha < 1$. In order to maintain the correct dimensions of the equation, we introduce a spacial parameter λ [13]. For $T = T(x, y, t)$, define

$$\nabla^\alpha T = \left[\bar{\delta} \frac{\partial^\alpha T}{\partial x^\alpha} - (1 - \bar{\delta}) \frac{\partial^\alpha T}{\partial (-x)^\alpha}, \ \bar{\delta} \frac{\partial^\alpha T}{\partial y^\alpha} - (1 - \bar{\delta}) \frac{\partial^\alpha T}{\partial (-y)^\alpha} \right],$$

where $\bar{\delta}$ ($0 \leqslant \bar{\delta} \leqslant 1$) is the weight coefficient of forward versus backward transition probability. The left and right Riemann–Liouville fractional derivatives of order α are defined as, respectively,

$$\frac{\partial^\alpha T}{\partial x^\alpha} = \frac{1}{\Gamma(1-\alpha)} \frac{\partial}{\partial x} \int_{x_1(y)}^{x} \frac{T(s, y, t)}{(x - s)^\alpha} \, ds,$$
$$\frac{\partial^\alpha T}{\partial (-x)^\alpha} = \frac{-1}{\Gamma(1-\alpha)} \frac{\partial}{\partial x} \int_{x}^{x_2(y)} \frac{T(s, y, t)}{(s - x)^\alpha} \, ds,$$

and similarly for $\partial^\alpha T / \partial y^\alpha$ and $\partial^\alpha T / \partial (-y)^\alpha$. Substituting the fractional derivative and the current density $\mathbf{J}$ into (3) gives the fractional equation

$$\rho C_p \frac{\partial T}{\partial t} = k \lambda^{\alpha - 1} \left[\left(\bar{\delta} \frac{\partial^{\alpha+1} T}{\partial x^{\alpha+1}} + (1 - \bar{\delta}) \frac{\partial^{\alpha+1} T}{\partial (-x)^{\alpha+1}} \right) + \left(\bar{\delta} \frac{\partial^{\alpha+1} T}{\partial y^{\alpha+1}} + (1 - \bar{\delta}) \frac{\partial^{\alpha+1} T}{\partial (-y)^{\alpha+1}} \right) \right] + \frac{\sigma B_0^2}{1 + \xi^2 B_0^2} w^2. \tag{4}$$

Due to the non-slip boundary conditions at the wall and the wall temperature T_w, the initial and boundary conditions are

$$\begin{aligned} &w(x, y, 0) = w_0(x, y), \quad T(x, y, 0) = T_0(x, y), \quad (x, y) \in \Omega, \\ &w(x, y, t) = 0, \quad T(x, y, t) = T_w, \quad (x, y) \in \partial\Omega, \quad t > 0, \end{aligned} \tag{5}$$

where w_0 and T_0 are the known smooth functions.

For convenience, dimensionless quantities are introduced:

$$x^* = \frac{x}{\lambda}, \quad y^* = \frac{y}{\lambda}, \quad t^* = \frac{\mu t}{\rho \lambda^2}, \quad w^* = \frac{\rho \lambda w}{\mu}, \quad \theta = \frac{T - T_w}{T_w},$$

$$w_0^* = \frac{\rho\lambda w_0}{\mu}, \quad \theta_0 = \frac{T_0 - T_w}{T_w}, \quad Ha^2 = \frac{\sigma B_0^2 \lambda^2}{\mu}, \quad m = \xi B_0,$$
$$Gr = \frac{g\eta T_w \rho^2 \lambda^3}{\mu^2}, \quad Pr = \frac{\mu C_p}{k}, \quad Br = \frac{\mu^2}{\rho^2 \lambda^2 T_w C_p},$$

where Ha is the Hartmann number, m is the Hall parameter, Gr is the thermal Grashof number, Pr is the Prandtl number, and Br is the Brinkmann number. We take $\bar{\delta} = 1/2$, and then the coupled equations (2) and (4) are rewritten as (dropping the asterisks)

$$\frac{\partial w}{\partial t} = \frac{\partial^2 w}{\partial x^2} + \frac{\partial^2 w}{\partial y^2} - \frac{Ha^2}{1+m^2} w - Gr\,\theta, \tag{6}$$
$$\frac{\partial \theta}{\partial t} = \frac{1}{2\,Pr}\left[\frac{\partial^{\alpha+1}\theta}{\partial x^{\alpha+1}} + \frac{\partial^{\alpha+1}\theta}{\partial(-x)^{\alpha+1}} + \frac{\partial^{\alpha+1}\theta}{\partial y^{\alpha+1}} + \frac{\partial^{\alpha+1}\theta}{\partial(-y)^{\alpha+1}}\right] + \frac{Br\,Ha^2}{1+m^2} w^2, \tag{7}$$

and the boundary conditions (5) are

$$w(x,y,0) = w_0(x,y), \quad \theta(x,y,0) = \theta_0(x,y), \quad (x,y) \in \Omega,$$
$$w(x,y,t) = 0, \quad \theta(x,y,t) = 0, \quad (x,y) \in \partial\Omega, \quad t > 0. \tag{8}$$

3 Numerical method

In order to study the general situation and test the effectiveness of the numerical method, we add the forcing terms $f_1(x,y,t)$ and $f_2(x,y,t)$ in equations (6) and (7), respectively. In the following discussion, we consider the 2D space fractional coupled equations

$$\frac{\partial w}{\partial t} = \frac{\partial^2 w}{\partial x^2} + \frac{\partial^2 w}{\partial y^2} - \frac{Ha^2}{1+m^2} w - Gr\,\theta + f_1(x,y,t), \tag{9}$$
$$\frac{\partial \theta}{\partial t} = \frac{1}{2\,Pr}\left[\frac{\partial^{\alpha+1}\theta}{\partial x^{\alpha+1}} + \frac{\partial^{\alpha+1}\theta}{\partial(-x)^{\alpha+1}} + \frac{\partial^{\alpha+1}\theta}{\partial y^{\alpha+1}} + \frac{\partial^{\alpha+1}\theta}{\partial(-y)^{\alpha+1}}\right] + \frac{Br\,Ha^2}{1+m^2} w^2 + f_2(x,y,t), \tag{10}$$

with boundary conditions (8).

For the irregular convex domain $\Omega \in \mathbb{R}^2$ shown in Figure 1, denote $x_{\min} = \min_{(x,y)\in\Omega} x_1(y)$, $x_{\max} = \max_{(x,y)\in\Omega} x_2(y)$, $y_{\min} = \min_{(x,y)\in\Omega} y_1(x)$, and $y_{\max} = \max_{(x,y)\in\Omega} y_2(x)$. In this work, we define the L^2-inner product in the irregular domain as the integral over Ω [5], and the L^2-norm as $\|u\|^2_{L^2(\Omega)} = (u,u)_{L^2(\Omega)}$.

For convenience of analysis and calculation, we define the notation

$$ {}_{x_1}D_x^{\alpha+1}\theta = \frac{\partial^{\alpha+1}\theta}{\partial x^{\alpha+1}}, \quad {}_xD_{x_2}^{\alpha+1}\theta = \frac{\partial^{\alpha+1}\theta}{\partial(-x)^{\alpha+1}}, $$

and the definitions of ${}_{y_1}D_y^{\alpha+1}\theta$ and ${}_yD_{y_2}^{\alpha+1}\theta$ are similar. Then we rewrite the space fractional derivatives as

$$ \frac{\partial^{\alpha+1}\theta}{\partial x^{\alpha+1}} + \frac{\partial^{\alpha+1}\theta}{\partial(-x)^{\alpha+1}} = {}_{x_1}D_x^{\alpha+1}\theta + {}_xD_{x_2}^{\alpha+1}\theta, $$

and $\partial^{\alpha+1}\theta/\partial y^{\alpha+1} + \partial^{\alpha+1}\theta/\partial(-y)^{\alpha+1}$ is similar.

Firstly, let $\widetilde{T}$ be the final time, τ be the time step and N be a positive integer, satisfying $\tau = \widetilde{T}/N$. Let $t_n = n\tau$, $n = 0, 1, \cdots, N$, $\mathbb{C}(\Omega)$ be the space of continuous functions on Ω, and $\mathbb{C}(\Omega \times (0, \widetilde{T}])$ be the space of continuous functions on $\Omega \times (0, \widetilde{T}]$. For the functions $w(x,y,t), \theta(x,y,t) \in \mathbb{C}(\Omega \times (0, \widetilde{T}])$, denote $w^n = w^n(x,y) = w(x,y,t_n)$ and $\theta^n = \theta^n(x,y) = \theta(x,y,t_n)$, and introduce the notation $D_1 w^n = (w^n - w^{n-1})/\tau$ and $D_1\theta^n = (\theta^n - \theta^{n-1})/\tau$. Then, we discretize temporal derivatives with the backward difference formulas $\delta w^n = D_1 w^n + O(\tau)$ and $\delta\theta^n = D_1\theta^n + O(\tau)$. For convenience, we derive the bilinear form [11]

$$ \begin{aligned} B(u,v) = -\Big[&\left({}_{x_1}D_x^{\frac{\alpha+1}{2}}u, {}_xD_{x_2}^{\frac{\alpha+1}{2}}v\right) + \left({}_xD_{x_2}^{\frac{\alpha+1}{2}}u, {}_{x_1}D_x^{\frac{\alpha+1}{2}}v\right) \\ &+ \left({}_{y_1}D_y^{\frac{\alpha+1}{2}}u, {}_yD_{y_2}^{\frac{\alpha+1}{2}}v\right) + \left({}_yD_{y_2}^{\frac{\alpha+1}{2}}u, {}_{y_1}D_y^{\frac{\alpha+1}{2}}v\right)\Big]. \end{aligned} \tag{11} $$

In particular, $B(u,v)$ is important for stability of the numerical method, and satisfies the following property [2].

Lemma 1. *For* $u \in H^{\gamma}(\Omega)$, *and* $\frac{1}{2} < \gamma < 1$, *the bilinear form* $B(u, v)$ (11) *satisfies* $B(u, u) \geqslant 0$.

Based on the formulas proposed by Feng et al. [6], we calculate $B(u, v)$, and obtain numerical solutions. Next, we give the full-discrete scheme and produce a weak formulation to solve the coupled model. Let $\{\mathcal{T}_h\}$ be a family of unstructured triangulations of Ω, and h be the maximum diameter of $\mathcal{T}_h$. Denote the finite element space

$$S_h = \{u_h : u_h \in \mathbb{C}(\Omega) \cap H_0^{\frac{\alpha+1}{2}}(\Omega), u_h|_E \in \mathbb{P}_s(E), \forall E \in \mathcal{T}_h\},$$

where $H_0^{\frac{\alpha+1}{2}}(\Omega)$ is the general Sobolev space and $\mathbb{P}_s(E)$ is the polynomial space in E with degree no more than s. Say w_h^n and θ_h^n are the finite element solutions at time $t = t_n$, and then we define the fully discrete scheme: find w_h^n and θ_h^n, such that for any $v \in S_h$ and $n \geqslant 1$:

$$\left(\frac{w_h^n - w_h^{n-1}}{\tau}, v\right) + (\nabla w_h^n, \nabla v) = -\frac{Ha^2}{1+m^2}(w_h^n, v) - Gr(\theta_h^{n-1}, v) + (I_h f_1^n, v), \tag{12}$$

$$\left(\frac{\theta_h^n - \theta_h^{n-1}}{\tau}, v\right) + \frac{1}{2\,Pr} B(\theta_h^n, v) = \frac{Ha^2\,Br}{1+m^2}((w_h^n)^2, v) + (I_h f_2^n, v), \tag{13}$$

with the initial conditions $w_h^0 = \Pi_h w^0$ and $\theta_h^0 = \Pi_h \theta^0$. Here, Π_h is the orthogonal projection operator satisfying $B(u - \Pi_h u, v) = 0$ for $u \in H_0^{\frac{\alpha+1}{2}}(\Omega)$ and $v \in S_h$. Incidentally, we calculate w_h^n using equation (12) firstly, and compute the non-linear term $((w_h^n)^2, v)$ directly.

4 Numerical example

4.1 Numerical implementation

For the unstructured triangulations of Ω, we define the nodes as $\{(x_l, y_l) : l = 1, 2, \ldots, N_p\}$, where N_p is the total number of nodes in the mesh. Let ϕ_k,

$k = 1, 2 \ldots, N_p$, be the basis functions satisfying $\phi_k(x_l, y_l) = \delta_{kl}$. Then the numerical solutions are $w_h^n = \sum_{i=1}^{N_p} w_k^n \phi_k(x, y)$ and $\theta_h^n = \sum_{i=1}^{N_p} \theta_k^n \phi_k(x, y)$. Taking $v = \phi_l(x, y)$ in equations (12)–(13), we have the matrix form

$$(\zeta_1^n M_B + \zeta_1^0 M_P)\boldsymbol{W}^n = \boldsymbol{F}_1^n, \tag{14}$$

$$(\zeta_2^n M_B + \zeta_2^0 M_A)\boldsymbol{\Theta}^n = \boldsymbol{F}_2^n, \tag{15}$$

in which

$$\begin{aligned}
&\zeta_1^0 = \tau, \quad \zeta_2^0 = \frac{\tau}{2\,\mathrm{Pr}}, \quad \zeta_1^n = 1 + \frac{\tau\,\mathrm{Ha}^2}{1+m^2}, \quad \zeta_2^n = 1, \quad n \geqslant 1,\\
&F_1^n(v) = (w_h^{n-1}, v) - \tau\,\mathrm{Gr}(\theta_h^{n-1}, v) + \tau(I_h f_1^n, v), \quad n \geqslant 1,\\
&F_2^n(v) = (\theta_h^{n-1}, v) + \frac{\tau\,\mathrm{Ha}^2\,\mathrm{Br}}{1+m^2}((w_h^n)^2, v) + \tau(I_h f_2^n, v), \quad n \geqslant 1.
\end{aligned}$$

Here $\boldsymbol{W}^n$ and $\boldsymbol{\Theta}^n$ are the vectors of w_k^n and θ_k^n, respectively, $M_B = (\phi_k, \phi_l)$, $M_P = (\nabla\phi_k, \nabla\phi_l)$ and $M_A = B(\phi_k, \phi_l)$ are the matrices of the basis functions [6], and $\boldsymbol{F}_i^n = (F_i^n(\phi_1), F_i^n(\phi_2), \cdots, F_i^n(\phi_{N_p}))$, $i = 1, 2$, are the vectors of nonlinear terms. The terms in $\boldsymbol{F}_1^n$ are explicit, so we solve equation (14) and obtain the numerical solution $\boldsymbol{W}^n$. We calculate $\boldsymbol{F}_2^n$ using the solution w^n, and then we solve equation (15) to obtain the numerical solution $\boldsymbol{\Theta}^n$.

4.2 Example

We consider a numerical example on the circle domain $\Omega = \{(x, y) : x^2 + y^2 \leqslant 1\}$ with exact solutions $w(x, y, t) = (2t + 1)e^x(x^2 + y^2 - 1)^2$ and $\theta(x, y, t) = (t^3 + 1)(x^2 + y^2 - 1)^2$. The coupled model with the boundary and initial conditions are

$$\begin{aligned}
\frac{\partial w}{\partial t} &= \frac{\partial^2 w}{\partial x^2} + \frac{\partial^2 w}{\partial y^2} - \frac{\mathrm{Ha}^2}{1+m^2} w - \mathrm{Gr}\,\theta + f_1(x, y, t),\\
\frac{\partial \theta}{\partial t} &= \frac{1}{2\,\mathrm{Pr}}\left[\frac{\partial^{\alpha+1}\theta}{\partial x^{\alpha+1}} + \frac{\partial^{\alpha+1}\theta}{\partial(-x)^{\alpha+1}} + \frac{\partial^{\alpha+1}\theta}{\partial y^{\alpha+1}} + \frac{\partial^{\alpha+1}\theta}{\partial(-y)^{\alpha+1}}\right] + \frac{\mathrm{Br}\,\mathrm{Ha}^2}{1+m^2} w^2\\
&\quad + f_2(x, y, t),
\end{aligned}$$

with

$$w(x,y,0) = e^x(x^2+y^2-1)^2\,, \quad \theta(x,y,0) = (x^2+y^2-1)^2\,, \quad (x,y) \in \Omega\,,$$
$$w(x,y,t) = 0\,, \quad \theta(x,y,t) = 0\,, \quad (x,y) \in \partial\Omega\,, \quad t > 0\,,$$

where $0 < \alpha < 1$, and the forcing terms

$$\begin{aligned}
f_1(x,y,t) = {} & -(2t+1)e^x\left[8x^2+8y^2+(x^2+y^2-1)^2+8(x+1)(x^2+y^2-1)\right] \\
& + \left[2+\frac{Ha^2(2t+1)}{1+m^2}\right]e^x(x^2+y^2-1)^2 + Gr(t^3+1)(x^2+y^2-1)^2\,, \\
f_2(x,y,t) = {} & 3t^2(x^2+y^2-1)^2 - \frac{Br\,Ha^2}{1+m^2}(2t+1)^2e^{2x}(x^2+y^2-1)^4 \\
& + \frac{t^3+1}{4\,Pr\cos((\alpha+1)\pi/2)}\left[(g_3(x,a_0,\alpha+1)+h_3(x,b_0,\alpha+1))\right. \\
& + (2y^2-2)\,(g_2(x,a_0,\alpha+1)+h_2(x,b_0,\alpha+1)) \\
& \left. + (y^4-2y^2+1)\,(g_1(x,a_0,\alpha+1)+h_1(x,b_0,\alpha+1))\right] \\
& + \frac{t^3+1}{4\,Pr\cos((\alpha+1)\pi/2)}\left[(g_3(y,c_0,\alpha+1)+h_3(y,d_0,\alpha+1))\right. \\
& + (2x^2-2)\,(g_2(y,c_0,\alpha+1)+h_2(y,d_0,\alpha+1)) \\
& \left. + (x^4-2x^2+1)\,(g_1(y,c_0,\alpha+1)+h_1(y,d_0,\alpha+1))\right].
\end{aligned}$$

Here

$$\begin{aligned}
& g_1(x,a,\gamma) = {}_aD_x^\gamma(1)\,, \quad g_2(x,a,\gamma) = {}_aD_x^\gamma(x^2)\,, \quad g_3(x,a,\gamma) = {}_aD_x^\gamma(x^4)\,, \\
& h_1(x,b,\gamma) = {}_xD_b^\gamma(1)\,, \quad h_2(x,b,\gamma) = {}_xD_b^\gamma(x^2)\,, \quad h_3(x,b,\gamma) = {}_xD_b^\gamma(x^4)\,, \\
& a_0 = -\sqrt{1-y^2}\,, \quad b_0 = \sqrt{1-y^2}\,, \quad c_0 = -\sqrt{1-x^2}\,, \quad d_0 = \sqrt{1-x^2}\,.
\end{aligned}$$

In this example, the parameters are chosen as $Ha = 1$, $m = 1$, $Gr = 0.5$, $Pr = 2$ and $Br = 0.7$. Figure 2 shows the unstructured triangular meshes. Figure 3 plots the exact solutions and numerical solutions of w and θ at $\widetilde{T} = 1$ for $\alpha = 0.5$, $h = 0.086550$ and $\tau = 1/1000$. The exact solutions

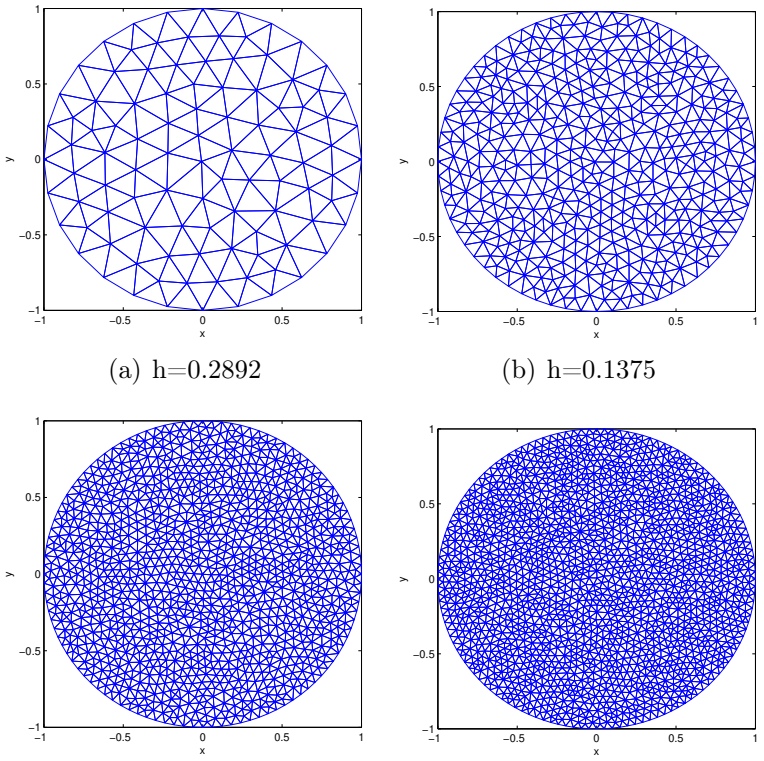

(a) h=0.2892 (b) h=0.1375

(c) h=0.0865 (d) h=0.0712

Figure 2: The unstructured triangular meshes.

and numerical solutions of w and θ fit well. Table 1 lists the L^2-error and convergence order of h for different α under $\tau = 1/1000$ and $\widetilde{T} = 1$. Table 2 exhibits the L^2-error and convergence order of τ, and we assume $\tau \approx h^2$. The numerical method attains first-order accuracy in time and second-order accuracy in space, so convergence is of $O(h^2+\tau)$. The numerical solutions are in excellent agreement with the exact solutions, and the presented numerical method is stable and efficient for solving this example of space fractional coupled equations for MHD flow.

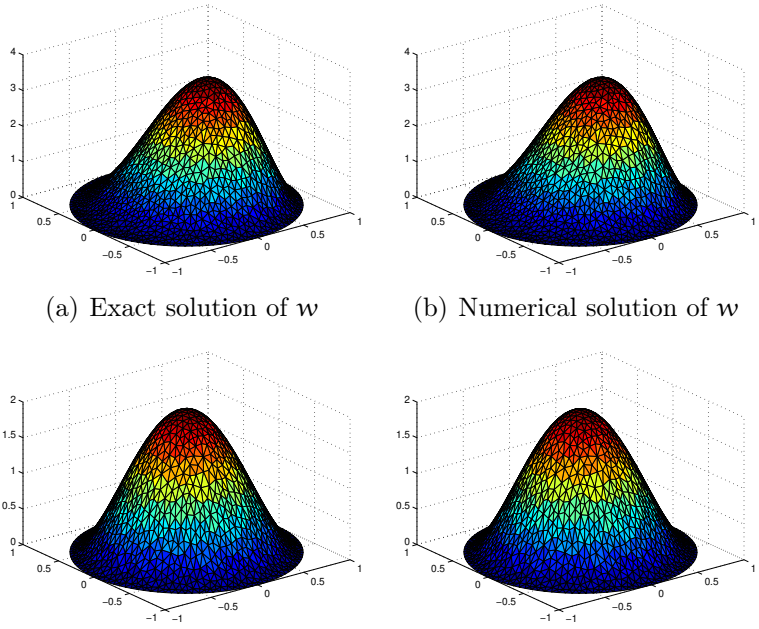

(a) Exact solution of w (b) Numerical solution of w

(c) Exact solution of θ (d) Numerical solution of θ

Figure 3: Exact solutions and numerical solutions of w and θ.

Table 1: The L^2-error and convergence order of h for different α.

α	$h\,(\times 10^{-1})$	N_g	N_e	w		θ	
				Error $(\times 10^{-2})$	Rate	Error $(\times 10^{-2})$	Rate
0.3	2.892	102	174	7.942	—	3.905	—
	1.375	467	868	2.015	1.845	1.011	1.818
	0.712	1793	3456	0.553	1.966	0.283	1.936
0.6	2.892	102	174	7.946	—	3.755	—
	1.375	467	868	2.016	1.845	0.950	1.849
	0.712	1793	3456	0.553	1.965	0.264	1.945

Table 2: The L^2-error and convergence order of τ for different α.

α	τ	N_g	N_e	w		θ	
				Error ($\times 10^{-1}$)	Rate	Error ($\times 10^{-1}$)	Rate
0.4	1/3	102	174	6.151	–	4.809	–
	1/7	467	868	2.471	1.077	2.663	0.698
	1/14	1793	3456	1.188	1.057	1.468	0.859
0.8	1/3	102	174	6.148	–	4.931	–
	1/7	467	868	2.468	1.077	2.707	0.708
	1/14	1793	3456	1.187	1.056	1.486	0.866

5 Conclusion

The MHD flow and heat transfer of a classical Newtonian fluid is modelled. By introducing a spatial fractional operator to modify the classical Fourier's law of thermal conduction, we obtain the space fractional coupled model. To solve the coupled model numerically, the unstructured mesh finite element method is proposed. Finally, a numerical example on a circular domain is conducted to verify the stability and the efficiency of the numerical method. From the results, the numerical scheme has accuracy of $O(\tau + h^2)$ when we choose L^2-error. For future work, we propose investigating how the efficient numerical method deals with other fractional coupled models on irregular domains.

Acknowledgements This research was supported by the Australian Research Council (DP190101889, DP230102414), National Natural Science Foundation of China (11801543, 12120101001), Natural Science Foundation of Shandong Province (ZR2021ZD03), and the State Scholarship Fund from China Scholarship Council (202106220102).

References

[1] S. Aman, Q. Al-Mdallal, and I. Khan. "Heat transfer and second order slip effect on MHD flow of fractional Maxwell fluid in a porous medium". In: *J. King Saud Uni. Sci.* 32.1 (2020), pp. 450–458. DOI: 10.1016/j.jksus.2018.07.007 (cit. on p. C63).

[2] W. Bu, Y. Tang, Y. Wu, and J. Yang. "Finite difference/finite element method for two-dimensional space and time fractional Bloch–Torrey equations". In: *J. Comput. Phys.* 293 (2015), pp. 264–279. DOI: 10.1016/j.jcp.2014.06.031 (cit. on p. C68).

[3] X. Chi and H. Zhang. "Numerical study for the unsteady space fractional magnetohydrodynamic free convective flow and heat transfer with Hall effects". In: *App. Math. Lett.* 120, 107312 (2021). DOI: 10.1016/j.aml.2021.107312 (cit. on p. C65).

[4] T. G. Cowling. *Magnetohydrodynamics*. New York: Interscience, 1957 (cit. on p. C65).

[5] W. Fan, F. Liu, X. Jiang, and I. Turner. "A novel unstructured mesh finite element method for solving the time-space fractional wave equation on a two-dimensional irregular convex domain". In: *Frac. Calc. Appl. Anal.* 20.2 (2017), pp. 352–383. DOI: 10.1515/fca-2017-0019 (cit. on p. C68).

[6] L. Feng, F Liu, I. Turner, Q. Yang, and P. Zhuang. "Unstructured mesh finite difference/finite element method for the 2D time-space Riesz fractional diffusion equation on irregular convex domains". In: *Appl. Math. Model.* 59 (2018), pp. 441–463. DOI: 10.1016/j.apm.2018.01.044 (cit. on pp. C69, C70).

[7] L. Feng, F. Liu, I. Turner, and L. Zheng. "Novel numerical analysis of multi-term time fractional viscoelastic non-Newtonian fluid models for simulating unsteady MHD Couette flow of a generalized Oldroyd-B fluid". In: *Frac. Calc. Appl. Anal.* 21.4 (2018), pp. 1073–1103. DOI: 10.1515/fca-2018-0058 (cit. on p. C63).

[8] C. Li and A. Chen. "Numerical methods for fractional partial differential equations". In: *Int. J. Comp. Math.* 95.6–7 (2018), pp. 1048–1099. DOI: 10.1080/00207160.2017.1343941 (cit. on p. C63).

[9] C. Li and F. Zeng. "Finite difference methods for fractional differential equations". In: *Int. J. Bifur. Chaos* 22.4, 1230014 (2012). DOI: 10.1142/S0218127412300145 (cit. on p. C63).

[10] Y. Liu, X. Chi, H. Xu, and X. Jiang. "Fast method and convergence analysis for the magnetohydrodynamic flow and heat transfer of fractional Maxwell fluid". In: *App. Math. Comput.* 430, 127255 (2022). DOI: 10.1016/j.amc.2022.127255 (cit. on p. C65).

[11] H. Zhang, F. Liu, and V. Anh. "Galerkin finite element approximation of symmetric space-fractional partial differential equations". In: *App. Math. Comput.* 217.6 (2010), pp. 2534–2545. DOI: 10.1016/j.amc.2010.07.066 (cit. on p. C68).

[12] H. Zhang, F. Zeng, X. Jiang, and G. E. Karniadakis. "Convergence analysis of the time-stepping numerical methods for time-fractional nonlinear subdiffusion equations". In: *Frac. Calc. Appl. Anal.* 25.2 (2022), pp. 453–487. DOI: 10.1007/s13540-022-00022-6 (cit. on p. C63).

[13] M. Zhang, M. Shen, F. Liu, and H. Zhang. "A new time and spatial fractional heat conduction model for Maxwell nanofluid in porous medium". In: *Comput. Math. Appl.* 78.5 (2019), pp. 1621–1636. DOI: 10.1016/j.camwa.2019.01.006 (cit. on pp. C65, C66).

[14] L. Zheng, Y. Liu, and X. Zhang. "Slip effects on MHD flow of a generalized Oldroyd-B fluid with fractional derivative". In: *Nonlin. Anal.: Real World Appl.* 13.2 (2012), pp. 513–523. DOI: 10.1016/j.nonrwa.2011.02.016 (cit. on p. C63).

Author addresses

1. **Yi Liu**, School of Mathematics, Shandong University, Jinan 250100, PR China, and School of Mathematical Sciences, Queensland University of Technology, GPO Box 2434, Brisbane, QLD 4001, Australia.
mailto:ytwzly@mail.sdu.edu.cn

2. **Xiaoyun Jiang**, School of Mathematics, Shandong University, Jinan 250100, PR China.
mailto:wqjxyf@sdu.edu.cn

3. **Fawang Liu**, School of Mathematical Sciences, Queensland University of Technology, GPO Box 2434, Brisbane, QLD 4001, Australia, and School of Mathematics and Statistics, Fuzhou University, Fujian 350108, PR China.
mailto:f.liu@qut.edu.au